Low-energy electronic properties of the AB-stacked few-layer graphites

2006 J. Phys.: Condens. Matter 18 5849

(http://iopscience.iop.org/0953-8984/18/26/005)

INSTITUTE OF PHYSICS PUBLISHING JOURNAL OF PHYSICS: CONDENSED MATTER

J. Phys.: Condens. Matter **18** (2006) 5849–5859 doi:10.1088/0953-8984/18/26/005

Low-energy electronic properties of the AB-stacked few-layer graphites

C L Lu[1], C P Chang[2,3], Y C Huang[1], J M Lu[4,5], C C Hwang[5] and M F Lin[1,3]

[1] Department of Physics, National Cheng Kung University, 701 Tainan, Taiwan
[2] Center for General Education, Tainan Woman's College of Arts and Technology, 710 Tainan, Taiwan
[3] National Center for Theoretical Sciences, 701 Tainan, Taiwan
[4] National Center for High-Performance Computing, No. 28, Nanke 3rd Road, Sinshih Township, Tainan County 744, Taiwan
[5] Department of Engineering Science, National Cheng Kung University, 701 Tainan, Taiwan

E-mail: t00252@ms.twcat.edu.tw (C P Chang)

Received 26 February 2006, in final form 29 April 2006
Published 16 June 2006
Online at stacks.iop.org/JPhysCM/18/5849

Abstract

In the presence of a perpendicular electric field, the low-energy electronic properties of the AB-stacked N-layer graphites with layer number $N = 2$, 3, and 4, respectively, are examined through the tight-binding model. The interlayer interactions, the number of layers, and the field strength are closely related to them. The interlayer interactions can significantly change the energy dispersions and produce new band-edge states. Bi-layer and four-layer graphites are two-dimensional semimetals due to a tiny overlap between the valence and conduction bands, while tri-layer graphite is a narrow-gap semiconductor. The electric field affects the low-energy electronic properties: the production of oscillating bands, the cause of subband (anti)crossing, the change in subband spacing, and the increase in band-edge states. Most importantly, the aforementioned effects are revealed completely in the density of states, e.g. the generation of special structures, the shift in peak position, the change in peak height, and the alteration of the band gap.

1. Introduction

The graphite-based family includes many members, for instance, one-dimensional (1D) nanotubes [1], zero-dimensional (0D) carbon toroids [2], 1D nanographite monoribbon [3, 4] and two-dimensional (2D) nanographite multiribbons [5]. Their physical properties have been amply studied for fundamental interest and possible applications. They exhibit a unique

characteristic, which strongly depends on the dimensionality and the size of the systems. 1D nanotubes can be treated as the rolling of a graphite sheet (graphene) into a cylinder system. The benzene rings of the carbon atoms with sp^2 orbitals form a 2D graphite sheet. Also, the remaining p_z orbitals perpendicular to the graphite plane dominate the peculiar low-energy electronic properties. A graphite sheet is a zero-gap semiconductor with two linear energy dispersions, which touch each other at the corners of the first Brillouin zone. A 0D carbon toroid is the connection of two ends of a finite 1D nanotube. A 1D nanographite ribbon is closer to a carbon nanotube. A nanoribbon is only an unrolled nanotube. Armchair and zigzag ribbons correspond to zigzag and armchair nanotubes, respectively [6]. 2D nanographite multiribbons (1D nanographite monoribbon) can alternatively be regarded as the slit of a graphite crystal (graphite sheet).

A graphite crystal is a vertical stack of hexagonal graphite sheets, united by the van der Walls forces, along the *c*-axis. A pile of graphite sheets in AA, AB, or ABC sequences results in 3D graphite crystals [7–9]. The interlayer interactions not only cause anisotropic energy dispersions along the stacking direction but also markedly change the energy dispersions at low energy [7–12]. The electronic properties of the 2D graphite sheet and 3D graphite crystals have been studied extensively for decades [13], and the geometric structures hold the key. For instance, a theoretical report of the magneto-electronic properties of a graphite sheet (the AB-stacked graphite) shows that geometric structures play an important role in the physical properties [14, 15]. More recently, the few-layer graphites (FLGs), which are piles of finite layers of graphite sheet along the *c*-axis, have been produced due to progress in fabrication techniques [16–19]. FLG-based devices, e.g. a field effect transistor, have also been fabricated [16]. FLG can be obtained, for example, through the exfoliation of a small mesa of highly oriented pyrolytic graphite. FLG is stable under ambient conditions. Transport measurements on these thin carbon films in the presence of a gating voltage exhibits that an FLG is a 2D semimetal with a light overlap between the valence bands and conduction bands [16]. These findings encouraged us to study electronic properties of FLGs theoretically.

Electric fields have been used to modify the electronic properties of low-dimensional systems, e.g. semiconducting 2D quantum wells, 2D superlattices, and 1D quantum wires. It is well known that an electric field significantly affects the electronic properties, magnetic properties, optical properties, and transport properties of these systems [20]. Furthermore, the effect of an electric field on the electronic properties of 1D carbon nanotubes has also been studied amply [21–25]. An electric field perpendicular to the tube axis considerably changes the electronic properties of nanotubes: modification of the energy dispersions; alteration of the band gap in the armchair tubes; and inducement of the metal–semiconductor transition. Carbon nanotubes may be a good candidate for electric-field-controlled switching devices. The above-mentioned studies reveal that the electric field can effectively alter both the electronic and transport properties of low-dimensional systems. It is expected that the novel electronic properties of FLG cannot be observed without an electronic field.

In this work, the electronic properties of FLGs with a layer number $N = 2$, 3, and 4 are explored within the tight-binding model. The dependence of electronic properties on the geometric structure (the number of layers and the interlayer interactions) and the electric field is investigated in detail. This paper is organized as follows. In section 2, the analytic Hamiltonian matrix elements of the tight-binding method for the electronic properties of FLGs are derived first and foremost. The effects of the geometric structure and the electric field on band dispersions are then investigated in section 3. Following this, the density of states (DOS) of FLG is studied. Finally, conclusions are drawn in section 4.

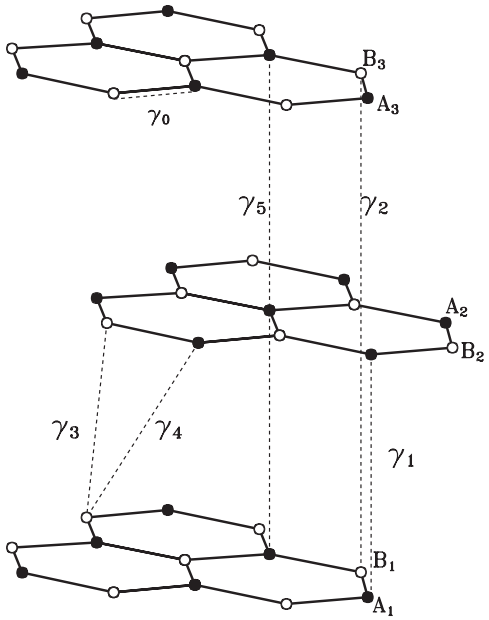

Figure 1. The geometric structure of the AB-stacked N-layer graphite with $N = 3$. γ_0 is the intralayer interaction and the γ_i s indicate the interlayer interactions.

2. The tight-binding method

The geometrical structure of AB-stacked N-layer graphite, for example with $N = 3$, is shown in figure 1. Two atoms, denoted as atom A and B, are found in the primitive cell of each graphite sheet. Hereafter, to distinguish each other, the atoms are labelled in italic type, i.e. atom A and atom B, and the normal type AB is used only for AB-stacked graphite. In the AB sequence, half the atoms lie directly above those in the adjacent sheets and the other half lie above the centre of the hexagons in the adjacent sheets. The primitive cell of N-layer graphite has $2N$ atoms ($A_1, B_1, A_2, B_2 \ldots A_N, B_N$). The system is periodic in each graphite sheet. Its first Brillouin zone is the same as that of graphene, as shown in the inset of figure 2(a). For the sake of calculation convenience, this FLG is treated as part of the AB-stacked graphite. Therefore, the geometric structure and all the tight-binding hopping integrals of the AB-stacked graphite can be used directly to simulate these FLG systems herein. The C–C bond length in the graphite plane is $b = 1.42$ Å. The distance between two nearest-neighbouring sheets is $c = 3.35$ Å [7]. The tight-binding hopping integrals of the AB-stacked graphite shown in figure 1 are as follows. That between A and B atoms on the same graphite sheet is γ_0. The hopping integral γ_1 (γ_3) is the interaction between two A (B) atoms from the two neighbouring sheets. γ_4 represents the interaction between atoms A and B from the two neighbouring sheets. γ_5 (γ_2) represents the interaction between two A (B) atoms from the two next-neighbouring sheets. The A atoms form linear atom chains along the stacking direction, while the B atoms form zigzag structures along that direction. Because of the special geometric structure, γ_5 is different from γ_2. Moreover, the local chemical environment of atom A is dissimilar to that of atom B. The chemical difference γ_6, due to the difference in the chemical environment between atoms A and B, is reflected in the site energy. The values of γ_0 and the γ_i s are [7]: $\gamma_0 = 2.598$ eV, $\gamma_1 = 0.364$ eV, $\gamma_2 = -0.014$ eV, $\gamma_3 = 0.319$ eV, $\gamma_4 = 0.177$ eV, $\gamma_5 = 0.036$ eV, and $\gamma_6 = -0.026$ eV.

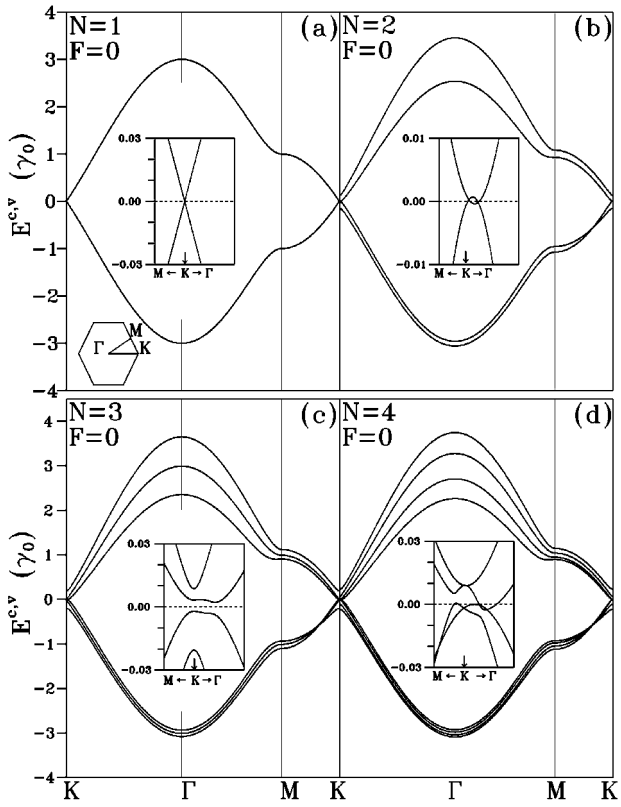

Figure 2. (a), (b), (c), and (d), respectively, exhibit energy dispersions of the AB-stacked N-layer graphite with $N = 1$, 2, 3, and 4 in the absence of an electric field. The insets show the low-energy dispersions.

Now, an electric field **F** perpendicular to the graphite sheets is applied to an FLG. The electric field is presumed not to affect the rigid structure and the tight-binding hopping integrals of the FLG. It merely adds an electric potential $U = -e\mathbf{F}z$ to the site energy of a carbon atom. Here, the field **F** is an effective field due to the screening effect. Notably, the main features of the electronic structures and the trend in the electronic properties of FLGs in the absence or presence of an electric field can still emerge clearly, even though these tight-binding hopping integrals are not modified. The Hamiltonian equation of the system is

$$H = \sum_i \epsilon_i(\mathbf{F}) C_i^+ C_i + \sum_{i,j,i\neq j} t_{i,j} C_i^+ C_j, \tag{1}$$

where i (j) denotes the atom sites. $\epsilon_i(\mathbf{F})$ is the field-modulated site energy of the carbon atom. C_i^+ (C_i) is the creation (annihilation) operator. $t_{i,j}$ is a hopping integral (γ_0, γ_1, γ_2, γ_3, γ_4, or γ_5). Only the π bands, which dominate the low-energy electronic properties, are included in the calculation. The σ bands which are far apart from the Fermi energy are omitted, for the low-energy dispersions are the only ones that interest us. After transferring the Hamiltonian equation into the matrix equation, the representation of an N-layer graphite in the presence of

the electric field is a $2N \times 2N$ Hermitian matrix:

$$\begin{pmatrix} H_{1,1} & H_2 & H_3 & 0 & \cdots & \cdots & 0 \\ H_2^* & H_{1,2}^* & H_2^* & H_3 & 0 & \cdots & 0 \\ H_3 & H_2 & H_{1,3} & H_2 & \ddots & \cdots & 0 \\ 0 & H_3 & \ddots & \ddots & \ddots & \cdots & 0 \\ 0 & 0 & \ddots & \ddots & \ddots & \ddots & \ddots \\ 0 & \vdots & 0 & \ddots & H_2^* & H_{1,N-1}^* & H_2^* \\ 0 & \cdots & \cdots & 0 & H_3 & H_2 & H_{1,N} \end{pmatrix}, \tag{2}$$

where $H_{1,i}$, H_2, and H_3 are 2×2 blocks. The occurrence of the complex conjugate in equation (2) is due to the special geometric structure of the AB-stacked few-layer graphites. The diagonal block $H_{1,i}$ is the Hamiltonian matrix of the ith graphite sheet along the z-axis. It is given by

$$H_{1,i} = \begin{pmatrix} -e\mathbf{F}z_i + \gamma_6 & \gamma_0 f(k_x, k_y) \\ \gamma_0 f^*(k_x, k_y) & -e\mathbf{F}z_i \end{pmatrix}, \tag{3}$$

where $-e\mathbf{F}z_i$ is the energy that results from the effective electric field and $z_i = (i-1) \cdot c$ is the z-coordinate of the ith graphite sheet. $f(k_x, k_y) = \sum_{l=1}^{3} \exp(\mathrm{i}\mathbf{k} \cdot \mathbf{b}_l)$. $\mathbf{b}_l$ represents the nearest neighbour in the same graphite sheet and $\mathbf{k} = (k_x, k_y)$ is the wavevector.

The off-diagonal block H_2 is:

$$H_2 = \begin{pmatrix} \gamma_1 & \gamma_4 f^*(k_x, k_y) \\ \gamma_4 f^*(k_x, k_y) & \gamma_3 f(k_x, k_y) \end{pmatrix}. \tag{4}$$

The hopping integrals γ_5 and γ_2, the second-neighbouring interactions, lead to the block H_3. It is

$$H_3 = \begin{pmatrix} \gamma_5 & 0 \\ 0 & \gamma_2 \end{pmatrix}. \tag{5}$$

Finally, the low-energy properties of N-layer graphite with $N \geqslant 3$ are found to be affected by the off-diagonal block H_3. Energy dispersions $E^{c,v}(k_x, k_y)$, in units of γ_0, are obtained through the diagonalization of the Hamiltonian matrix, where c (v) represents the unoccupied (occupied) states. The DOS of N-layer graphite is then calculated from the energy dispersions.

3. Electronic properties

In order to see the physical properties change from a graphite sheet to multilayer graphite, we choose FLGs with layer numbers of $N = 1, 2, 3$, and 4 for the purpose of systematic study. The energy dispersions in the absence of an effective electric field ($\mathbf{F} = 0$) are shown in figure 2. Only the graphite sheet exhibits symmetric bands, where the occupied states E^v are symmetric to the unoccupied states E^c about the Fermi level (E_F) (figure 2(a)). The more layers that the FLG has, the wider the band width is. Apparently, the main features of the energy bands are very sensitive to the geometric structure (the number of layers and the interlayer interactions).

The low-energy dispersions are also shown in the insets of figure 2, where E_F (indicated by the dashed line) is pinned to zero. The linear bands only exist in the graphite sheet (the inset of figure 2(a)). Two linear bands cross each other at the K point. A graphite sheet is a zero-gap semiconductor. Above all, these two linear bands are absent in FLG systems (the insets of figures 2(b)–(d)). It should be noted that tri-layer graphite is a semiconductor with a narrow band gap, while the other FLGs are 2D semimetals. In short, the interlayer interactions can cause asymmetry between the occupied states E^v and the unoccupied states E^c, enhance

the band width, destroy the symmetry and isotropy of the energy bands, and change the linear bands into parabolic bands.

The dependence of low-energy electronic properties on the interlayer interactions and layer number is discussed in detail. The state energies of bi-layer graphite at the K point can be obtained analytically by diagonalizing a 4×4 Hamiltonian matrix, which only includes the nearest-neighbouring interactions (appendix). These are $E = 0$ and $E = \gamma_6 \pm \gamma_1$. Around the K point (the inset of figure 2(a)), the interlayer interactions (γ_3 and γ_4) not only apparently change the linear bands into parabolic bands but also significantly cause the overlap between the valence and conduction bands. The low-energy dispersions of tri-layer graphite show oscillating energy dispersions near E_F (the inset of figure 2(c)). Notably, a narrow band gap is opened up. Analytic state energies at the K point (appendix) show that the interactions γ_2 and γ_5 greatly influence the low-energy properties of tri-layer graphite. As shown in the inset of figure 2(d), the low-energy dispersions of the four-layer graphite exhibit a quite dissimilar characteristic. At the K point, the state energies of the highest occupied state (the lowest unoccupied state) are doubly degenerate. The energy spacing between the two degenerate states is equal to $2|\gamma_2|$ (see appendix). Along KΓ (KM), the state degeneracy is destroyed and the energy dispersions are dramatically altered. The valence bands have light overlap with the conduction bands. Thus, four-layer graphite is a 2D semimetal. The findings reveal that the layer number decides the low-energy electronic properties of FLG.

The perpendicular electric field significantly modulates the low-energy dispersion of FLGs (figure 3). It should be noted that E_F in figures 3(a)–(f) is always pinned to zero. Finally, the effective electric field, in units of $\gamma_0/(e$ Å), alters the band features, opens up a band gap, causes the subband (anti)crossing, changes the band spacing, and produces new band-edge states as well. The electric field can, remarkably, open up a band gap and cause the semimetal–semiconductor transition in bi-layer graphite (the bold curves in figure 3(a)). The size of the band gap E_g of bi-layer graphite varies with the field strength F (figure 3(b)). In contrast to bi-layer graphite, the E_g of tri-layer graphite shrinks with an increase in field strength (figure 3(c)) and finally closes up at a critical field strength (figure 3(d)). As a result, a semiconductor–semimetal transition occurs in tri-layer graphite. Moreover, the electric field causes oscillating band dispersions and, thus, produces new band-edge states near E_F. It is expected that the features of energy bands (the oscillating band dispersions and the band-edge states) will influence the DOS of FLGs.

The origins of the oscillating band dispersions and band-edge states are dwelt upon alternately. Take bi-layer graphite, for example. The closing up of the interlayer interactions leads to two sets of linear bands (the light curves in figure 3(a)), which are the energy dispersions of two independent graphite sheets in the presence of the electric field. Apparently, the electric field shifts the state energies and removes the state degeneracy. It also causes the band crossing. As a result, oscillating energy dispersions occur near E_F. There are many band-edge states. As shown by the bold curves in figure 3(a), the energy dispersions are immensely modified in the presence of the interlayer interactions, which cause the anticrossing between the low-energy bands, then change the linear bands into parabolic bands, alter the positions of band-edge states, and finally open up a band gap. Above all, the features of the low-energy dispersions of FLG are significantly dominated by the field strength and crystal potentials (the intralayer and interlayer interactions).

The size of the band gap E_g, which is quite sensitive to the field strength F, deserves closer investigation (figure 4). The transition from semimetal to semiconductor is induced by an electric field in bi-layer and four-layer graphites, while the semiconductor–semimetal transition occurs in tri-layer graphite. In the bi-layer graphite system, E_g first grows linearly with an increase in the field strength F, and is still increasing at the maximum field. As to

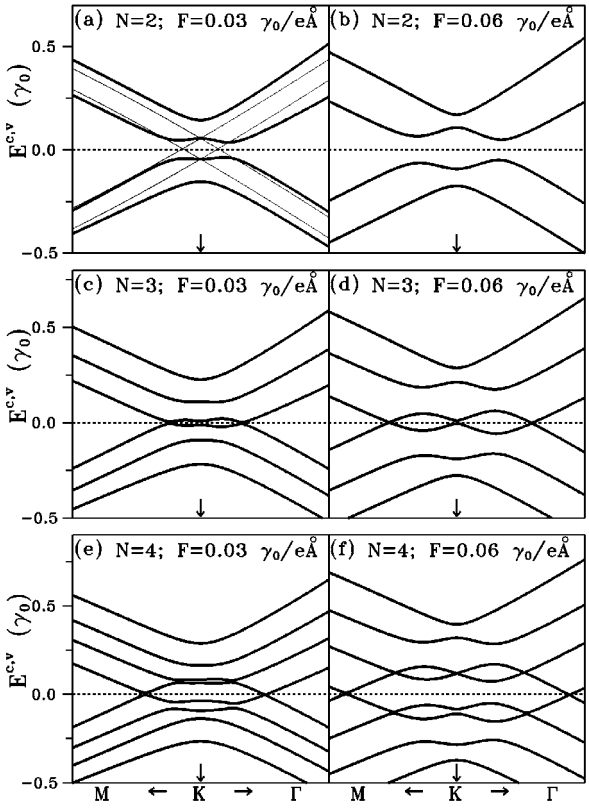

Figure 3. Energy dispersions of AB-stacked N-layer graphite in the presence of an electric field are exhibited for $N = 2$, 3, and 4, respectively.

tri-layer and four-layer graphites, E_g exhibits a quite different feature as the field strength varies. The fact that E_g is not equal to zero in the absence of an electric field clearly indicates that tri-layer graphite is a semiconductor. The E_g of tri-layer graphite first increases with the field strength and then reaches a maximum value. Finally, it declines to zero. Thus, a semiconductor–semimetal transition occurs. In the absence of an electric field, four-layer graphite is a semimetal. Its E_g is opened up when the field strength is greater than a threshold value. E_g first reaches a maximum value and then slows down to zero as the field strength increases.

Now, the properties of band structures are also revealed in the DOS, which is evaluated from $D(\omega) = \sum_{\mathbf{k},h} |\nabla_{\mathbf{k}} E^h(\mathbf{k};\phi)|^{-1}_{E^h=\omega}$. In the absence of an electric field, the DOS of FLGs, as shown in figures 5(a) and (b), mainly exhibits two kinds of special structures: discontinuities and logarithmic divergences, which are, respectively, due to the band-edge states and the saddle points in the energy bands (figures 2(a)–(d)). However, the DOS features are very sensitive to the geometric structure. The DOS of a graphite sheet, as shown by the light dashed curve in figure 5(a), is symmetric about $\omega = 0$ and is featureless at $|\omega| > \gamma_0$. Logarithmic divergences take place at $\omega = \pm\gamma_0$, respectively. The DOS is asymmetric about $\omega = 0$ as the FLG layer number increases. Around $\omega = \gamma_0$ ($\omega = -\gamma_0$) there are N logarithmic divergences. Their peak positions (peak heights) are not symmetric about $\omega = 0$.

As shown in figure 5(b), the DOS in the low-energy region is easily influenced by a change in layer number. In contrast to the featureless DOS of the graphite sheet, there are many

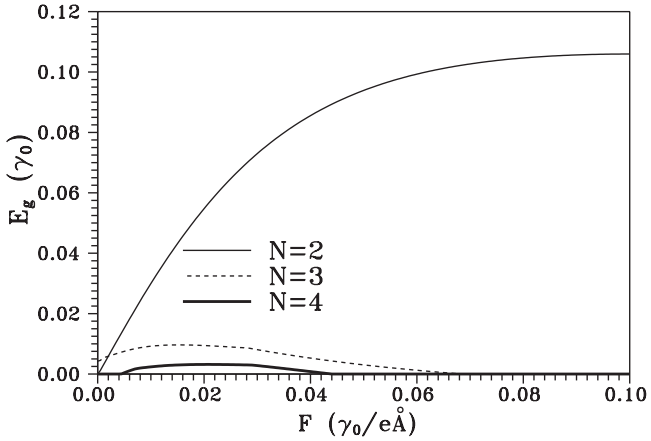

Figure 4. The band gap, E_g, of AB-stacked N-layer graphite ($N = 2$, 3, and 4) versus field strength F.

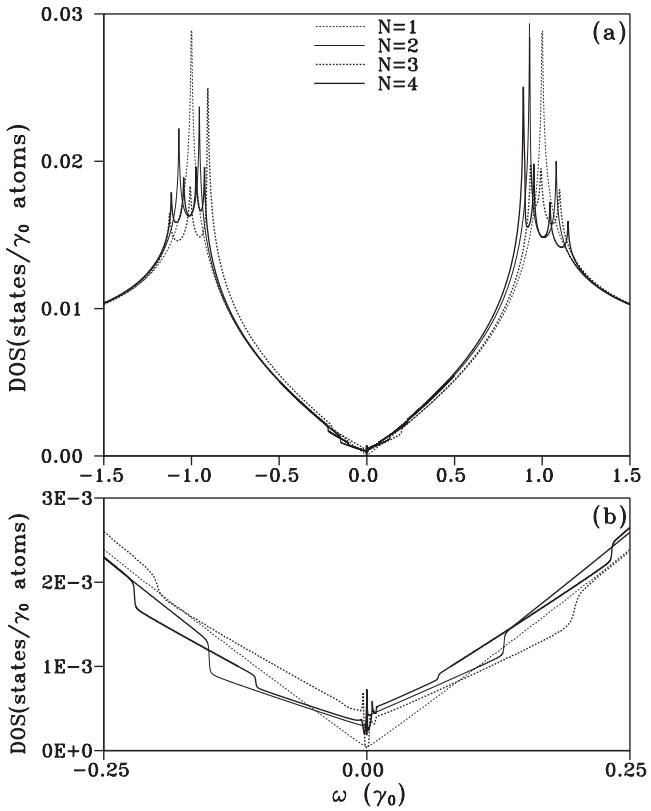

Figure 5. (a) The light dashed, light solid, bold dashed, and bold solid curves show the DOS of $N = 1$, 2, 3, and 4 FLGs in the absence of an electric field, respectively. (b) The low-energy DOS.

jump structures in the DOS of FLGs, which are related to the band-edge states (the insets of figures 2(b)–(d)). Moreover, a graphite sheet is a zero-gap semiconductor with a vanishing DOS at $\omega = 0$. Such a unique feature originates specifically in the linear bands (figure 2(a)).

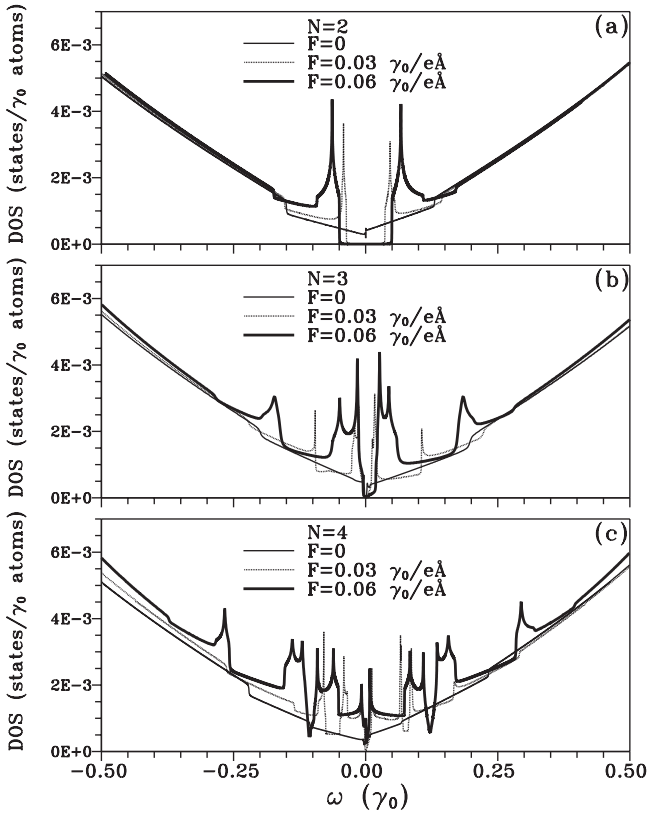

Figure 6. The low-energy DOS of $N = 2$, 3, and 4 FLGs in the presence of an electric field are shown, respectively, in (a), (b), and (c).

However, bi-layer and four-layer graphites exhibit a non-zero DOS at $\omega = 0$, caused by the tiny overlap between the conduction and valence bands (figures 2(b) and (d)). A band gap is found in the DOS of tri-layer graphite.

An electric field greatly affects the DOS features in the low-energy region (figure 6). The DOS chiefly exhibits discontinuities and the logarithmic divergences, which are related to band-edge states and oscillating dispersions in the energy bands, respectively (figure 3). Besides, the more layers that the FLG has, the more peaks that the DOS will present. The peak position and peak feature, as we can see, clearly rely on the field strength F (figures 6(a)–(c)). It is worthwhile noting that the electric field also opens up a band gap in bi-layer graphite (figure 6(a)). As a result, the transition from semimetal to semiconductor is induced by the electric field.

The dependence of the electronic properties of FLGs on the options of the tight-binding parameters is discussed. There are several sets of tight-binding parameters of AB-stacked graphite reported in the literature (e.g. the set proposed by Nygen-Manh [26]). No matter which set of tight-binding parameters we employ, the main features of the energy dispersions of FLGs, such as the local minimum and local maximum at the K point, the parabolic bands at the M point, and the maximum and minimum at the Γ point, can be shown in the energy dispersions, i.e. the main features of the energy bands are independent of the parameters that we adopt. The chief differences in energy dispersions caused by the variation of parameters are the band width and the state energies at the Γ and M points. It is remarkable that the

characteristics of the low-energy dispersions in the vicinity of the K point are preserved when a different set of parameter is used. The chief cause is that the low-energy dispersions are mainly dominated by γ_2, γ_5 and γ_6 (appendix). Most importantly, the magnitudes of parameters γ_2, γ_5 or γ_6 from the different sets are close in value. In other words, the features of the low-energy electronic properties are not sensitive to the tight-binding parameters that we employ.

The relevance of the present results to the experimental results is stated. Experimentally, FLGs, including monolayer, bi-layer and tri-layer graphites, are found to be a hole metal in the absence of an electric field [16], which is attributed to unintentional doping of the film by absorbed water. Moreover, the electric field doping effect is found to change a hole metal to a complete hole or complete electron conductor. Theoretically, the low-energy electronic properties of FLG are explored in this work. All FLGs studied here are pure, clean and intrinsic. No adsorpants and no dopants are introduced into the systems. The electric field doping effect is not taken into consideration in the calculation. The main contribution of this study is that the low-energy electronic properties of FLGs are strongly dependent on the geometrical structures (the layer number and interlayer interactions) and the magnitude of the electric field. Due to the difference between these two systems, no comparison of the experimental results with the theoretical results can be made directly. To study the effect, caused by the adsorption or the dopant, on the electronic properties of FLG is the topic of future work.

4. Conclusions

In this work, low-energy electronic properties of AB-stacked N-layer graphites, where $N = 2$, 3, and 4, are studied intensively within the tight-binding model. The dependence of the electronic properties on the geometric structure (the number of layers and the interlayer interactions) and the strength of the effective electric field is explored. In the absence of an electric field, bi-layer and four-layer graphites are semimetals, while tri-layer graphite is a semiconductor. The interlayer interactions destroy the symmetry and isotropy of the energy bands and change the linear bands into parabolic bands. Remarkably, they also cause a weak overlap between the valence and conduction bands in bi-layer and four-layer graphites. The analytical electronic properties at the K point are helpful in understanding the effect caused by geometric structures. The switch-on of a perpendicular electric field can produce oscillating energy bands, open up a band gap, cause subband (anti)crossing, change the subband spacing, and increase the band-edge states. Most importantly, the effects, caused by the geometric structure and electric field, are revealed completely in the DOS, e.g. two kinds of special structures, an increase in peak numbers, a shift of peak position, a change in peak height, and an alteration of the band gap.

Acknowledgments

The authors gratefully acknowledge the support of the Taiwan National Science Council under contract numbers NSC 94-2112-M-165-001 and NSC 94-2112-M-006-0002.

Appendix

The Hamiltonian matrix of bi-layer graphite is a 4×4 matrix:

$$H = \begin{pmatrix} \gamma_6 & \gamma_0 f(k_x, k_y) & \gamma_1 & \gamma_4 f^*(k_x, k_y) \\ \gamma_0 f^*(k_x, k_y) & 0 & \gamma_4 f^*(k_x, k_y) & \gamma_3 f(k_x, k_y) \\ \gamma_1 & \gamma_4 f(k_x, k_y) & \gamma_6 & \gamma_0 f^*(k_x, k_y) \\ \gamma_4 f(k_x, k_y) & \gamma_3 f^*(k_x, k_y) & \gamma_0 f(k_x, k_y) & 0 \end{pmatrix}. \tag{6}$$

At the K point, $f(k_x, k_y)$ is equal to zero and the Hamiltonian matrix is reduced to a simple form:

$$H = \begin{pmatrix} \gamma_6 & 0 & \gamma_1 & 0 \\ 0 & 0 & 0 & 0 \\ \gamma_1 & 0 & \gamma_6 & 0 \\ 0 & 0 & 0 & 0 \end{pmatrix}. \tag{7}$$

Eigenvalues can be obtained analytically. The state energies are $E = 0$ and $E = \gamma_6 \pm \gamma_1$. Similarly, the eigenvalues of the tri-layer graphite at the K point are $E = 0, \pm\gamma_2, \gamma_6 - \gamma_5$, and $(\gamma_5 + 2\gamma_6 \pm \sqrt{6\gamma_1^2 + \gamma_5^2})/2$. The state energies, plotted in figure 2, are rearranged according to the Fermi level, E_F, which is pinned to zero. As to four-layer graphite, the eigenvalue of the lowest unoccupied (highest occupied) state, which is doubly degenerate, is $E = \gamma_2$ ($E = -\gamma_2$) at the K point.

References

[1] Satio R, Dresselhaus G and Dresselhaus M S 1998 *Physical Properties of Carbon Nanotubes* (London: Imperial College Press)
[2] Rocha C G, Pacheco M, Barticevic Z and Latge A 2004 *Phys. Rev.* B **70** 233402
[3] Nakada K, Fujita M, Dresselhaus G and Dresselhaus M S 1996 *Phys. Rev.* B **54** 17954
[4] Wakabayashi K, Fujita M, Ajiki H and Sigrist M 1999 *Phys. Rev.* B **59** 8271
[5] Chiu C W, Shyu F L, Chang C P, Chen R B and Lin M F 2003 *J. Phys. Soc. Japan* **72** 170
[6] Iijima S 1991 *Nature* **354** 56
[7] Charlier J C, Gonze X and Michenaud J P 1991 *Phys. Rev.* B **43** 4579
[8] Charlier J C, Michenaud J P and Gonze X 1992 *Phys. Rev.* B **46** 4531
[9] Charlier J C, Gonze X and Michenaud J P 1994 *Carbon* **32** 289
[10] Ahuja R, Auluck S, Trygg J, Wills J M, Eriksson O and Johansson B 1995 *Phys. Rev.* B **51** 4813
[11] Tatar R C and Rabii S 1982 *Phys. Rev.* B **25** 4126
[12] Mendez M, Misu A and Dresselhaus M S 1980 *Phys. Rev.* B **21** 827
[13] Kelly B T 1981 *Physics of Graphite* (London: Applied Science)
[14] Chang C P, Lu C L, Shyu F L, Chen R B, Fang Y K and Lin M F 2004 *Carbon* **42** 297
[15] Chang C P, Lu C L, Shyu F L, Chen R B, Huang Y C and Lin M F 2005 *Carbon* **43** 1424
[16] Novoselov K S *et al* 2004 *Science* **306** 666
[17] Bunch J S, Yaish Y, Brink M, Bolotin K and McEuen P L 2005 *Nano Lett.* **5** 287
[18] Wu Y H, Yang B J, Zong B Y, Sun H, Shen Z X and Feng Y P 2004 *J. Mater. Chem.* **14** 469
[19] Zhang Y, Small J P, Pontius W V and Kim P 2005 *Appl. Phys. Lett.* **86** 073104
[20] Singh J 1993 *Physics of Semiconductors and their Heterostructures* (New York: McGraw-Hill)
[21] Kim Y H and Chang K J 2001 *Phys. Rev.* B **64** 153404
[22] O'Keeffe J, Wei C Y and Cho K J 2002 *Appl. Phys. Lett.* **80** 676
[23] Li Y, Rotkin S V and Ravaioli U 2003 *Nano Lett.* **3** 183
[24] Khoo K H, Mazzoni M S C and Louie S G 2004 *Phys. Rev.* B **69** 201401
[25] Pacheco M, Barticevic Z, Rocha C G and Latge A 2005 *J. Phys.: Condens. Matter* **17** 5839
[26] Nygen-Manh D, Saha-Dasgupta T and Anderson O K 2003 *Bull. Mater. Sci.* **26** 27